

## AN ABSTRACT OF THE THESIS OF

Robyn O. Faber for the degree of Master of Science in Materials Science and Engineering presented on November 20, 1998. Title: Dwell Time Low Cycle Fatigue in Ti-6242Si.

Abstract approved: **Redacted for Privacy**

---

Michael E. Kassner

Dwell time low cycle fatigue (DLCF), low cycle fatigue (LCF), and creep tests were performed at ambient temperature on Ti-6Al-2Sn-4Zr-2Mo-0.1Si (Ti-6242Si). Test specimens were solution annealed at various temperatures below the beta transus to control the volume fraction of primary alpha. The influence of the changes in primary alpha phase on low cycle dwell time fatigue life were determined and compared to the conventional low cycle fatigue properties of the alloy. A dwell period significantly decreased the number of cycles to failure, but by a decreasing factor with decreasing stress. The increased primary alpha phase present associated with lower solution anneal temperatures significantly increased susceptibility to low cycle dwell time fatigue. It is believed that dwell fatigue sensitivity may be associated with cyclic, ambient temperature, time-dependent plasticity (creep).

Dwell Time Low Cycle Fatigue in Ti-6242Si

by

Robyn O. Faber

A THESIS  
submitted to  
Oregon State University

in partial fulfillment of  
the requirements for the  
degree of  
Master of Science

Completed November 20, 1998  
Commencement June 1999

Master of Science thesis of Robyn O. Faber presented on November 20, 1998

APPROVED:

Redacted for Privacy

\_\_\_\_\_  
Major Professor, representing Materials Science

Redacted for Privacy

\_\_\_\_\_  
Coordinator of Materials Science Program

Redacted for Privacy

\_\_\_\_\_  
Dean of Graduate School

I understand that my thesis will become part of the permanent collection of Oregon State University libraries. My signature below authorizes release of my thesis to any reader upon request.

Redacted for Privacy

\_\_\_\_\_  
Robyn O. Faber, Author

## ACKNOWLEDGEMENT

I would like to acknowledge and thank OREMET - WAH CHANG, and the Oregon Joint Schools of Engineering for their financial assistance and overall support. I would also like to acknowledge the assistance of Yoji Kasaka and Bryan Bristow at OREMET - WAH CHANG, and the insight of Dr. M. E. Kassner at Oregon State University. Finally, I would like to acknowledge the assistance of Dr. Karol Schrems at the Albany Research Center with the metallography, and Dr. Xiao Li with the creep testing.

## TABLE OF CONTENTS

	<u>Page</u>
INTRODUCTION .....	1
REVIEW OF LITERATURE .....	6
EXPERIMENTAL PROCEDURE .....	10
RESULTS .....	19
DISCUSSION .....	34
CONCLUSIONS .....	37
REFERENCES .....	38
APPENDIX .....	41

## LIST OF FIGURES

<u>Figure</u>	<u>Page</u>
1. Alpha (primary $\alpha$ and transformed $\beta$ ) + Beta Microstructure consisting of approximately 97% $\alpha$ and 3% $\beta$ .....	3
2. Widmanstätten Microstructure .....	4
3. Flow Chart for TMP Ingot to Billet Conversion .....	11
4. The Instron 8521 with Sample Loaded for a DLCF Test .....	16
5. DLCF and LCF Testing Profiles .....	17
6. Ti-6242Si Dwell & Low Cycle Fatigue Data .....	20
7. DLCF and LCF Results for IMI 685 as Reported by W.J. Evans [13] .....	21
8. RT950209, Set B, Sample T2TOP1, $T_{\beta}$ -53° C, Axial Section .....	22
9. RT950209, Set B, Sample T2TOP4, $T_{\beta}$ -41° C, Transverse Section .....	23
10. RT950522, Set A, Sample #2, $T_{\beta}$ -28° C, Transverse Section .....	24
11. RT950483, Set A, Sample #1, $T_{\beta}$ -28° C, Transverse Section .....	25
12. RT950209, Set B, Sample T2TOP6R, $T_{\beta}$ -14° C, Transverse Section .....	26
13. RT950209, Set B, Sample T2TOP22, $T_{\beta}$ - 3° C, Transverse Section .....	27
14. RT950209, Set B, Sample T2TOP18OH, Unknown Solution Anneal Temperature, Estimated $T_{\beta}$ - 8° C, Transverse Section .....	28
15. Ti-6242Si Creep Data (Ambient temperature, Constant Engineering Stress Tests) ..	30
16. DCF / LCF / Creep Testing Sample Dimensions / Specifications .....	42
17. DCF Sampling, Preparation, and Testing Outline .....	43

## LIST OF FIGURES (continued)

<u>Figure</u>	<u>Page</u>
18. Plot of Set A and Metcut Research, Inc. Dwell Cycle Fatigue Data .....	44
19. Ti-6242Si, Heat RT950209 Solution Anneal Temperatures vs. UTS .....	45

## LIST OF TABLES

<b><u>Table</u></b>	<b><u>Page</u></b>
1. Ingot Compositions (wt %) .....	12
2. Heat Treatment Table for OREMET-WAH CHANG Ti-6242Si Test Specimens..	14
3. Summary of Average Primary Alpha and Hardness for Each Solution Anneal Temperature .....	29
4. Ambient Temperature Creep Data for Ti-6242Si.....	31
5. Tensile Properties of Ti-6242Si as a Function of Solution Anneal Temperature .....	33
6. Set A Specimen List and Data .....	46
7. Set B Specimen List and Data .....	47



## INTRODUCTION

Dwell sensitivity refers to the reduction in fatigue life as a result of adding a holding time, or dwell period, at peak load to a low cycle fatigue (LCF) test. This dwell time low cycle fatigue (DLCF) test better simulates actual service conditions of aircraft turbine engine components typically made from titanium alloys. Ti-6Al-2Sn-4Zr-2Mo-0.1Si (Ti-6242Si), a near alpha, alpha-beta alloy, is one such alloy used in aerospace and aeronautical, high temperature applications. One specific use for Ti-6242Si is for aircraft turbine engine compressor disks.

Ti-6242Si consists of primarily a hexagonal close packed (hcp) crystallographically structured alpha phase plus three percent or less body centered cubic (bcc) beta phase at room temperature. The transformation temperature above which the one hundred percent beta phase is thermodynamically stable is referred to as the beta transus ( $T_\beta$ ). The added aluminum acts as an alpha phase stabilizer, the molybdenum as a beta phase stabilizer, and the zirconium and tin as solid solution strengthening agents as well as transformation rate retardants. The added silicon maximizes creep resistance through dispersion strengthening and the resulting stabilization of the surface engineering properties during elevated temperatures under stress [1, 2].

An alpha-beta ( $\alpha$ - $\beta$ ) alloy is one where a mixture of alpha and beta phases exists at equilibrium, usually room temperature [2]. The “near- $\alpha$ ” designation refers to an  $\alpha$ + $\beta$  composition containing less than three percent beta [3], and, therefore, is near the  $\alpha$ / $\alpha$ + $\beta$  phase boundary [2]. Two forms of alpha phase are typically present, primary alpha and transformed beta. The primary alpha is that which remains in the alpha phase throughout heat treatment. Transformed beta is alpha phase which changes to beta during heat treatment above the beta transus, then returns to alpha upon cooling [3]. This alpha may emerge as acicular or lamellar, serrated, platelike, or Widmanstätten in appearance [3]. Widmanstätten microstructure is described as coarse colonies of aligned alpha platelets [2]. Heat treatments are a means of “adjusting” the microstructure to control the properties of alpha-beta alloys [2].

The microstructures most common for Ti-6242Si are  $\alpha$  (primary  $\alpha$  and transformed  $\beta$ ) +  $\beta$ , and acicular  $\alpha$  (Widmanstätten or basketweave) plus  $\beta$ . The former is a microstructure of equiaxed alpha phase (primary  $\alpha$ ) in a transformed beta matrix (Fig.1), and is produced through heat treatment below the beta transus and slow cooling. This microstructure is referred to as  $\alpha$  +  $\beta$ , has good high temperature fatigue properties, and is a stable microstructure [4]. Furnace cooling produces this coarse, aligned alpha structure which some have suggested is particularly sensitive to dwell cycle fatigue [5, 6]. Heat treatment above the beta transus results in a Widmanstätten, aligned acicular, alpha microstructure upon cooling (Fig. 2), and is known to have good high temperature creep properties [4]. As the cooling rate from above the beta transus is increased, the transformed beta becomes finer, and a basketweave microstructure is produced [7].

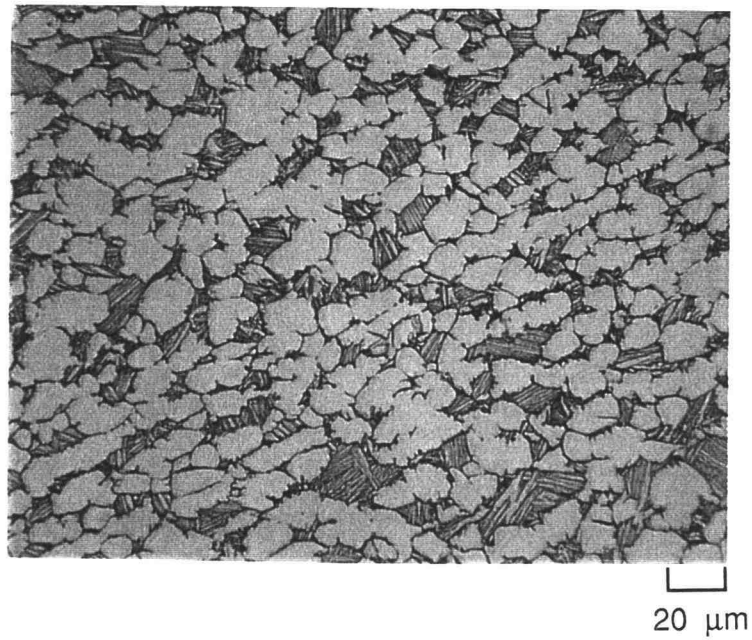


Figure 1. Alpha (primary  $\alpha$  and transformed  $\beta$ ) + Beta Microstructure  
consisting of approximately 97%  $\alpha$  and 3%  $\beta$

(The above micrograph is of a Ti-6242Si specimen tested during this study)

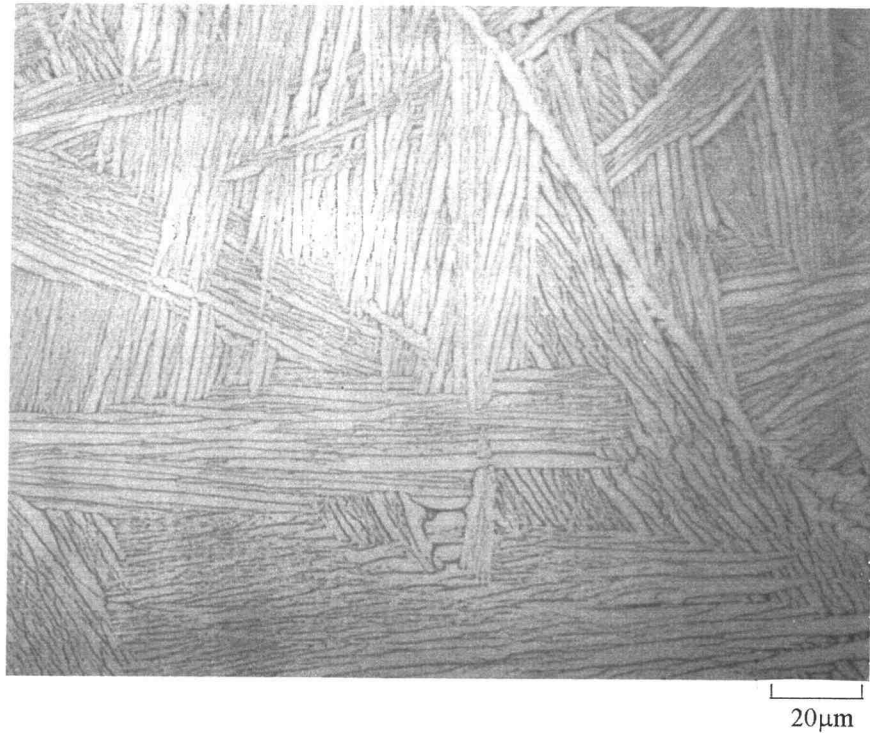


Figure 2. Widmanstätten Microstructure

(The above micrograph is of a Ti-6242Si specimen tested during this study)

Basketweave microstructure is reported to be the least susceptible to dwell cycle fatigue by simple virtue of a more “tortuous” crack propagation path, but processing to attain it is unreasonable in an industrial situation [6]. The cooling rate from above the beta transus, therefore, significantly affects the alloy’s mechanical properties by altering the microstructure [1].

The objective of the present work was to confirm the existence of a dwell debit in near-alpha Ti-6242Si, produced by alpha/beta processing, and investigate the effectiveness of solution anneal temperature changes in reducing this debit. Solution annealing allows for accurate and consistent temperature control in an industrial situation as it is accomplished after thermomechanical processing the titanium in its largest form. Studying factors affecting dwell cycle fatigue life may also aid in the determination of the fundamental mechanism of dwell fatigue.

## REVIEW OF LITERATURE

Dwell sensitivity can result in over an order of magnitude fewer cycles to failure, and was first reported by J. Waisman et al. in 1973 [8]. Work has been continued by Evans and coworkers, Eylon and Hall [9], and Woodfield et al. [5]. Most studies have focused on the titanium alloy IMI 685 or Ti-6-4, but the most recent works cite results of tests using a number of titanium alloys, including Ti-6242Si, or exclusively Ti-6242Si.

The mechanism leading to dwell sensitivity is still unresolved. In 1979, Evans and Gostelow [10] suggested that ambient temperature dwell sensitivity is due to time-dependent plastic strain accumulation, and that facet formation during creep deformation is linked to the extensive facet formation present in dwell cycle fatigue specimens [10].

“Titanium alloys have the intrinsic property to creep at ambient temperature [11].”<sup>1</sup> In 1984, Chu et al. found that a dwell period leads to stress relaxation, which has the same effect as prior creep [11]. Chu’s group also reported that multiple (fifty or more) fatigue cycles between hold times actually results in a longer life when compared to low cycle fatigue results. The given explanation that prior creep increases the resistance of the material through the delaying of fatigue damage (hardening) is contradictory to Evans and Gostelow, but Chu et al. also reported that only one cycle between hold times did

---

<sup>1</sup> H.P. Chu, B.A. MacDonald, and O.P. Arora, *Titanium Science and Technology*, Vol. 4, Eds. G. Lütjering, U. Zwicker, and W. Bunk, Proceedings of the 5<sup>th</sup> International Conference on Titanium, Deutsche Gesellschaft für Metallkunde, E.V., Munich, 1984, p. 2395.

not generate interaction between fatigue and prior creep during that investigation, and a reduction in fatigue life with the added strain-hold time was observed [11].

The microstructure of Ti-6242Si can be altered by changing the solution anneal temperature below the beta transus ( $T_\beta$ ). This affects the amounts of primary alpha and transformed beta present, and may affect the dwell sensitivity in two ways. First, the amount of primary alpha, which increases with decreasing solution anneal temperature, could change the strength of the alloy. Second, this would tend to alter plasticity, and, perhaps, affect the susceptibility to dwell effects according to the time-dependent plasticity (creep) explanation.

In 1988, Neal published a number of findings after performing low cycle and dwell cycle fatigue tests on various titanium alloys, including Ti-6242Si. He explained the presence of a dwell effect at temperatures below approximately 200° C by means of planar slip on or near the hcp basal plane (0001), and by creep-fatigue interactions at temperatures above approximately 400° C. His explanation for the lack of dwell sensitivity between these two temperatures is dynamic strain aging.

Suri and coworkers reported in 1997 that “extensive low temperature, primary creep in titanium alloys is clearly associated with extreme planar slip.”<sup>2</sup>

---

<sup>2</sup> S. Suri, T. Neeraj, G.S. Daehn, D.H. Hou, J.M. Scott, R.W. Hayes, and M.J. Mills, *Materials Science and Engineering*, A234-236, 1997, pp. 996-999.

Thiehse et al. reported in 1992 that “raising the solution anneal temperature increases both the primary and steady state, high temperature creep resistance of Ti-6242Si. The beneficial effect may be derived from a combination of several sources, including the removal of such micrographic features as banding or texturing, and especially the altering or refining of the  $\alpha$  or  $\beta$  microstructure.”<sup>3</sup>

Hack and Leverant reported in 1982 that “beta-processed, near-alpha titanium alloys with a large colony microstructure were found to be susceptible to internal hydrogen embrittlement under conditions of sustained loading of fatigue cycling with a dwell period at peak load.”<sup>4</sup> A colony is described as a cluster of acicular alpha grains aligned in the same orientation [3]. Their study found that both time-dependent deformation and internal hydrogen are required for the embrittlement to occur. Hydrogen embrittlement occurs by localized increases in hydrogen content at the tips of long, blocked shear bands developed during time dependent plastic deformation [12]. Fatigue crack nucleation is a result of cyclic loading which causes to-and-fro slip to occur [13]. When this slip results persistent slip bands, then extrusions and intrusions result. Cracks are thought to nucleate at intrusions [14]. Woodfield et al. presented results indicating that thermomechanical processing can “break up” the aligned alpha colonies creating randomly orientated primary alpha [5]. Increasing the final solution anneal temperature closer to the beta transus, followed by quenching, can not only alter the volume fraction of primary alpha, but may also decrease the possibility of any aligned alpha colonies. Reduction of susceptibility to DLCF may result through simply minimizing the volume

---

<sup>3</sup> K.E. Thiehse, M.E. Kassner, J. Pollard, D.R. Hiatt, and B. Bristow, *Metall. Trans.*, 24A, 1993, p. 1819.

<sup>4</sup> J.E. Hack and G. R. Leverant, *Metall. Trans.*, 13A, 1982, p. 1729.



of the weaker alpha phase or by reducing the alpha colonies thought to be associated with the facets linked to internal DLCF crack initiation [5].

Evan's 1987 paper reports that his results do not support the shear band model, and, in contrast, suggests that there is an increase in life with hydrogen content [8]. He also states that once the cracks are formed, though, their growth is greatly influenced by hydrogen concentration. Previous work [6, 10, 12] has shown that times to failure for creep and dwell tests with a five minute holding period per cycle are indistinguishable. Evans said that the mechanisms responsible for crack initiation are the same for creep, dwell, and cyclic fatigue testing, and that they probably involve time-dependent strain accumulation.

Neal's findings that almost identical dwell effects were present at all levels of hydrogen tested, including a degassed material ( $<10$  ppm  $H_2$ ), were also in contrast to those reported by Hack and Leverent. In addition, Neal stated that "because both alpha/beta and beta heat treated structures exhibited dwell effects, alloying composition appeared the controlling factor. Hack and Leverent suggested Ti-6242Si was not susceptible to dwell effects, even when beta heat treated,"<sup>5</sup> and that microstructural features associated with the hydrogen embrittlement process are the key to DLCF in IMI 685 [12]. Furthermore, Neal found that the higher the stress, the greater the percentage cyclic life loss with a dwell period added [15].

---

<sup>5</sup> D.F. Neal, Sixth World Conference on Titanium, Vol. 1, Proceedings of the Sixth World Conference on Titanium, Cannes, 1988, p. 175.

## EXPERIMENTAL PROCEDURE

Standard thermomechanical processing (TMP) was applied to 914 mm diameter Ti-6242Si ingots which, in turn, were forged to approximately 238 mm diameter round billets. Five to six billets result from a single ingot. Rectangular coupons were cut from an ingot position designated billet with the long axis of the coupons radial to the long axis of the billet, and so that the specimen gage section would be at approximately the mid-radius position.

All specimens are identified by the heat number of the OREMET-WAH CHANG production billet from which the sample coupons were extracted as well as by the position designation along that billet (Fig. 3). The beta transus for each billet was determined by differential thermal analysis (DTA). The ingot chemical compositions are presented in Table 1, and were determined by inductively coupled plasma atomic emission spectroscopy (ICP) and gas analysis. The specific processing steps follow.

- The ingot was heated initially to 1149° C, upset (set up on end which results in the compression of the ingot to a specified amount) by approximately fifty percent, and forged to dimensions 813 mm x 1067 mm x L.
- This was followed by a forging to 737 mm square, also after heating to 1149° C, and a water quench.

FIGURE 3. Flow Chart for TMP Ingot to Billet Conversion

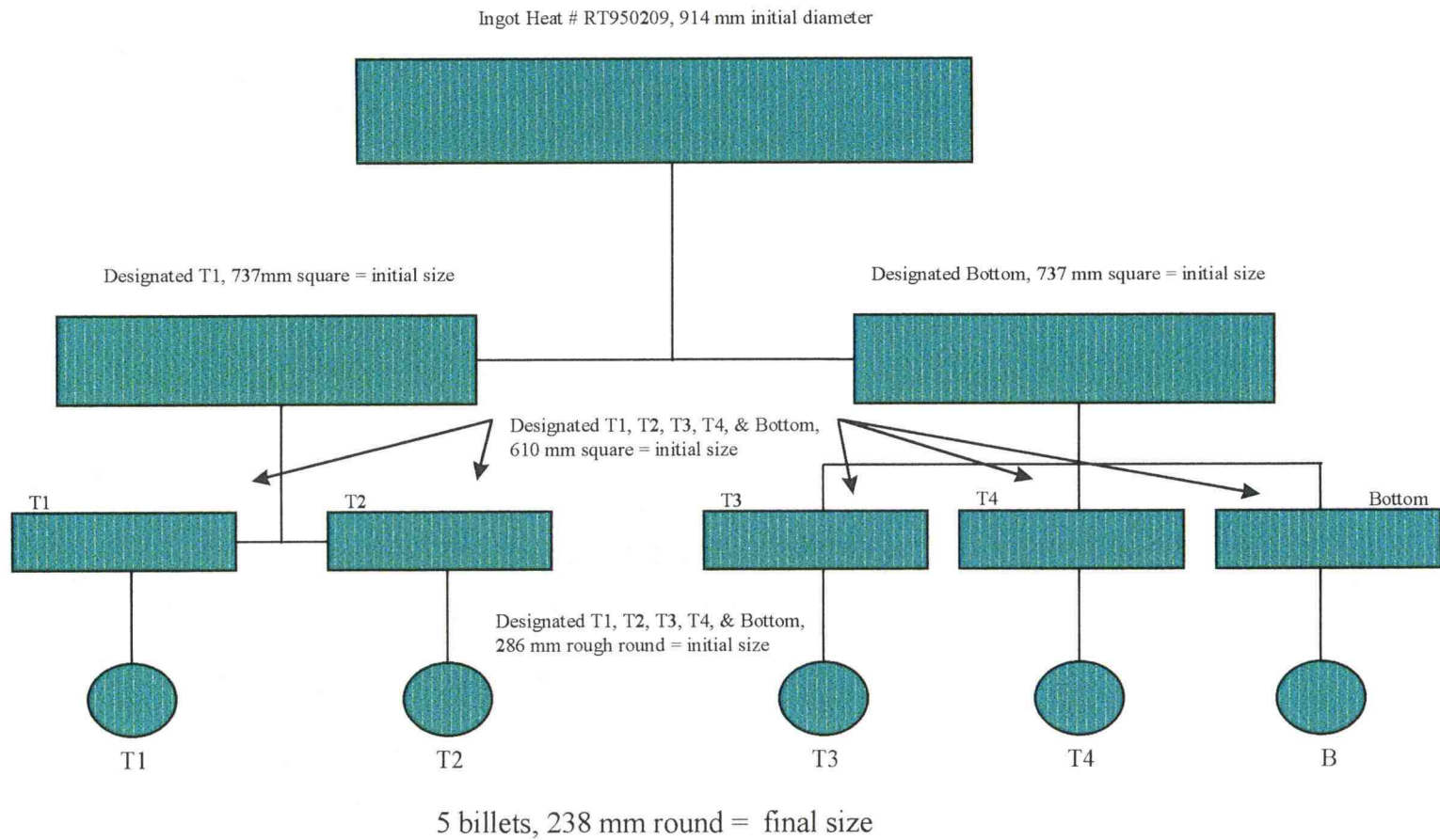


Table 1. Ingot Compositions (wt %)

		Al	Cr	Fe	Mo	Ni	Si	Sn	Zr	C	O	N	H
RT950209 $T_{\beta} = 1007^{\circ}\text{C}$ (DTA)	Top	6.08	0.003	0.033	2.00	0.007	0.09	2.01	4.18	0.005	0.107	0.002	0.0044
	Bottom	6.00	0.002	0.033	1.95	0.007	0.09	1.96	4.09	0.003	0.104	0.001	0.0047
RT950483 $T_{\beta} = 1007^{\circ}\text{C}$ (metall.)	Top	6.3	0.002	0.031	2.01	0.008	0.09	2.02	4.17	0.005	0.133	0.001	—
	Bottom	5.93	0.002	0.03	1.94	0.007	0.08	1.91	4.04	0.006	0.13	0.001	0.0060
RT950522 $T_{\beta} = 1007^{\circ}\text{C}$ (metall.)	Top	6.08	0.001	0.032	2.05	0.001	0.08	1.99	4.12	0.004	0.127	0.002	—
	Bottom	5.99	0.001	0.033	1.96	0.001	0.09	1.93	4.13	0.009	0.123	0.003	0.0045

- The alloy was then forged to 610 mm square after heating to 954° C. Next, it was heated to 1066° C, which is above the beta transus, and held at that temperature for two hours before water quenching.
- After heating to 968° C and forging to 286 mm rough round, the billet was conditioned (cosmetic surface grinding), heated again to 968° C, and forged by rotary forging machine to 238 mm round. Solution annealing at 954° C for two hours forty-two minutes and air cooling followed.
- Finally the billet was annealed at 704° C for six to nine hours, air cooled, and peeled (descaled). The rectangular coupons were cut from the billet after this step.

Solution heat treating of the coupons ( $T_{\beta} - 3^{\circ}\text{C}$  to  $T_{\beta} - 53^{\circ}\text{C}$ ) for one hour followed by an eight hour age, as outlined in Table 2, preceded machining and surface treating. All solution heat treating, machining, and surface treating was completed by Metcut Research, Inc., Dickson Testing Company, Inc., or a combination of both companies. The final specimens have an average gage diameter of 6.3 mm, and a gage length of 19 mm. All gage sections were peened using S-110, S-170, CW-14, or CW-33 shot to 0.002 - 0.008 A, 100% to 400% coverage [16]. Hardness testing was performed at Oregon State University using the Rockwell C test.

All tests, fatigue and creep, were performed using an 8521 Instron at Oregon State University. This Instron is a digitally controlled, servohydraulic, biaxial testing machine with a maximum load capability of 20,000 pounds. The attached control panel allows for precise monitoring, general programming, and rapid response times. An additional

**TABLE 2. HEAT TREATMENT TABLE FOR OREMET-WAH CHANG TI - 6242Si TEST SPECIMENS**

<b>BILLET HEAT IDENTIFICATION SAMPLE IDENTIFICATION</b>	<b>SOLUTION ANNEAL</b>	<b>AGING</b>	<b>PROCESSING LAB</b>
RT950483, RT950522 A 483 #1 & #2, and A 522 #1 & #2	979° C $\pm$ 14° for 1 hr., cool at 17° C / min $\pm$ 3° to below 538° C	593° C $\pm$ 8° for 8 hrs., air cool	Dickson Testing Company, Inc.
RT950209 A T2TOP1 through A T2TOP14, and Manila #2	966° C $\pm$ 14° for 1 hr., cool at 17° C / min $\pm$ 3° to below 538° C	593° C $\pm$ 8° for 8 hrs., air cool	Metcut Research, Inc. (T2TOP1-14) Dickson Testing Company, Inc. (Manila #2)
RT950209 B T2TOP1 & 2	954° C for 1 hr., cool at 17° C / min. to 593° C	hold at 593° C for 5 hrs., air cool	Metcut Research, Inc.
RT950209 B T2TOP21, 22, & 23	1004° C for 1 hr., cool at 17° C / min. to 593° C	hold at 593° C for 8 hrs., air cool	Metcut Research, Inc.
RT950209 B T2TOP1R through 13R	993° C for 1 hr., cool at 17° C / min. $\pm$ 3° to below 538° C	593° C $\pm$ 8° for 8 hrs., air cool	Dickson Testing Company, Inc.
RT950209 B T2TOP7OH through 20OH,	Beta Transus exceeded. Most samples returned untested	593° C $\pm$ 8° for 8 hrs., air cool	Metcut Research, Inc.

computer with Labview software was used for more specific programming and data collection during the creep tests.

Prior to testing, each specimen was cleaned with acetone, then two strain gages were mounted 180 degrees apart in the same position along the longitudinal axis of the gage section. Strain indicators wired to the gages were used to maintain zero strain on the sample during installation into the grips on the Instron. The Instron was programmed to maintain zero load during this process. This careful installation and alignment procedure, coupled with a grip designed to minimize possible bending stresses, resulted in highly reproducible results and minimum scatter (Fig. 4).

The low cycle fatigue (LCF) testing cycle consisted of a two second loading period to peak followed immediately by a two second unloading period back to zero load. The testing cycle for the dwell cycle fatigue tests also consisted of a two second loading to peak load, but was followed by a two minute hold time at that peak load before the two second unloading to zero (Fig. 5). All testing was performed at a stress ratio,

$R = \sigma_{\min} / \sigma_{\max} = 0$ . All values of stress and strain are reported as engineering stress and strain.

During the ambient temperature creep tests, the Instron was programmed to maintain a constant load for approximately twenty-four hours with the attached computer monitoring and collecting strain data from the mounted strain gages. The loading time to the desired stress was sixty seconds.

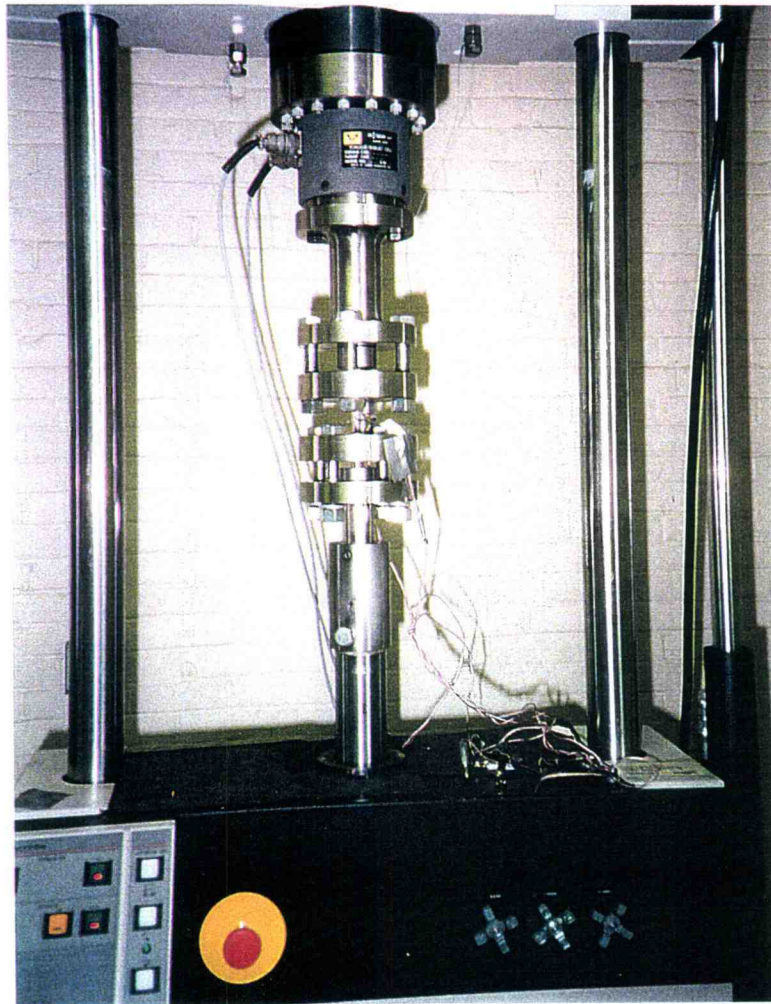
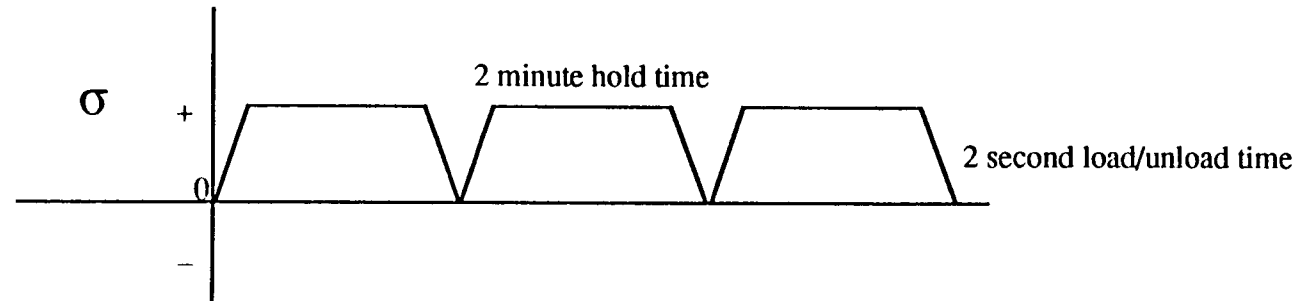


Figure 4. The Instron 8521 with Sample Loaded for a DCF Test



### DWELL TIME LOW CYCLE FATIGUE



### LOW CYCLE FATIGUE

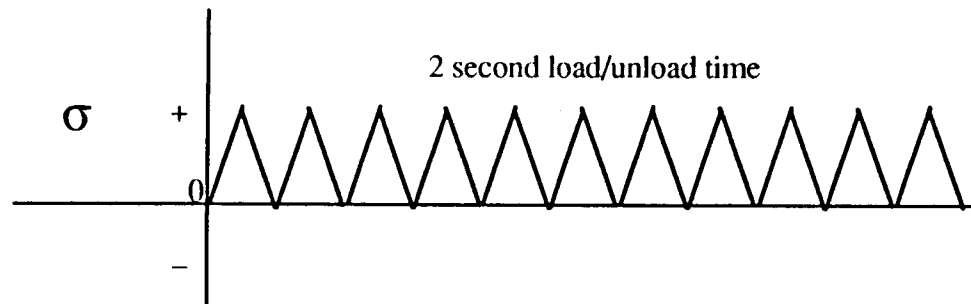


Figure 5. DLCF and LCF Testing Profiles

After testing, axial and transverse sections were taken from specimens using a diamond blade on a low speed saw, then mounted in phenolic powder, ground, and polished. All polishing was accomplished using  $\text{SiO}_2$  suspension solution after grinding on 320, 400, and 600 grit silicon carbide grinding paper. The samples were then etched with a ten percent HF, fifteen percent  $\text{HNO}_3$ , and seventy-five percent  $\text{H}_2\text{O}$  etchant (Kroll's reagent) for approximately three seconds. Area fractions of primary alpha were calculated using NIH Image Analysis computer software after scanning in micrographs taken with an Olympus PME optical microscope.

## RESULTS

Figure 6 presents the results obtained through low cycle fatigue testing as well as dwell cycle fatigue testing in the form of a stress versus log number of cycles to failure plot. The corresponding legend identifies each set of data, the solution anneal temperature for that set, and the type of test (LCF or DLCF). Again, Table 2 lists the heat treatments for each set of Ti-6242Si specimens. The plot of data in Figure 6 clearly shows the reduction in the number of cycles to failure as a result of the added two minute dwell period. This reduction is by over an order of magnitude number of cycles at the most elevated stresses, decreasing to a factor of five at the lowest tested stresses. It is probable that the dwell cycle fatigue curves merge with the low cycle fatigue data line at lower stresses than were tested during this investigation. These results are generally consistent with those published by Evans (Fig. 7) [8]. Micrographs illustrating the typical microstructure (and volume percent primary alpha) developed by each solution anneal temperature are pictured in Figures 8 through 14. It is clear that the dwell cycle fatigue cycles to failure increase with increasing solution anneal temperature or decreasing volume percent primary alpha. Table 3 gives a summary of the average primary alpha phase present and average hardness data for the associated solution anneal temperatures.

Figure 15 contains a plot of ambient temperature creep tests in the form of creep strain versus time in seconds for a given engineering stress, and, expectedly, displays higher creep strains per unit of time with higher solution anneal temperatures. Table 4 contains this creep strain data for each solution anneal temperature and tested stress.

Figure 6. TI-6242Si Dwell & Low Cycle Fatigue Data

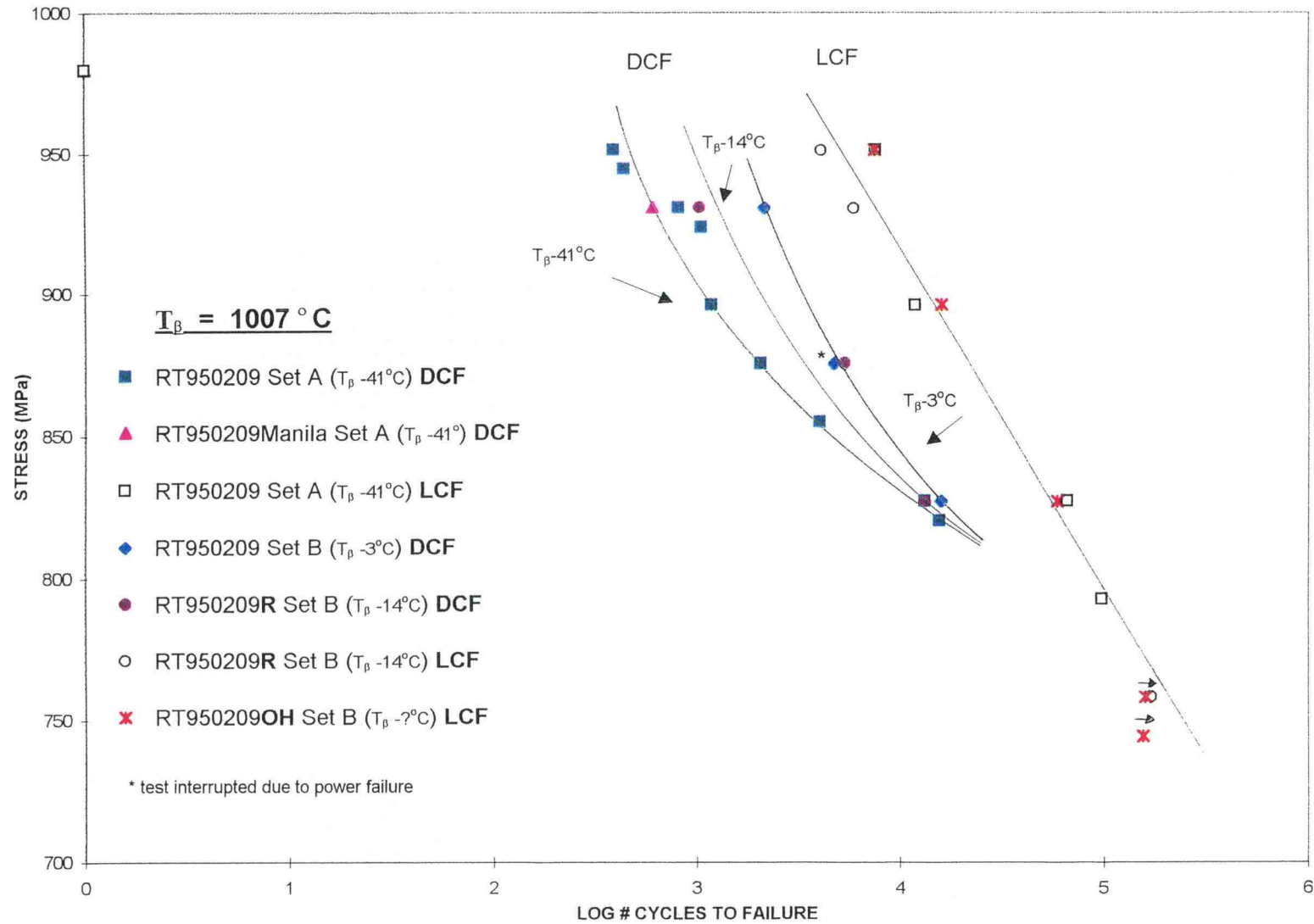
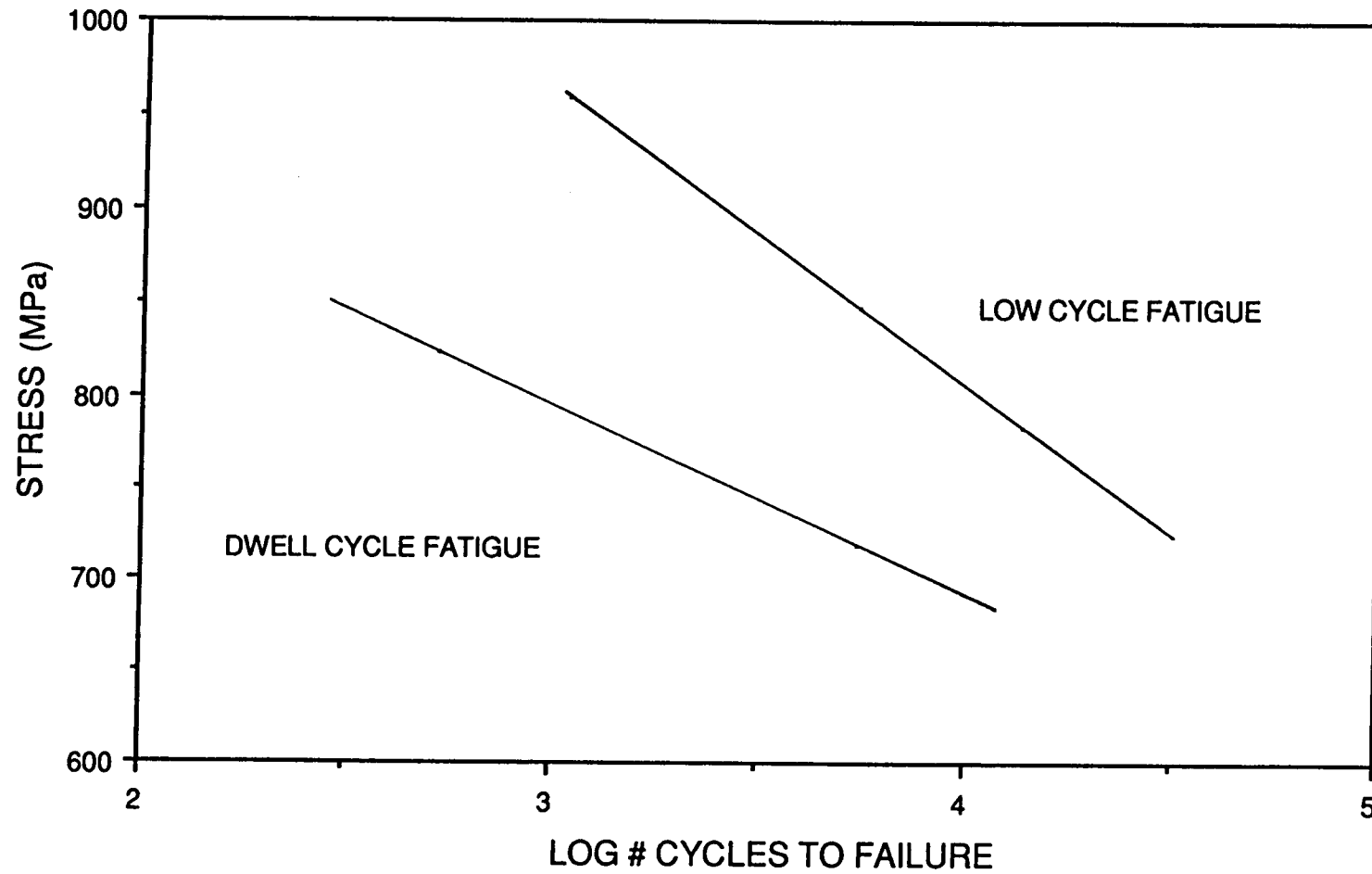


Figure 7. DLCF and LCF Results for IMI 685 as Reported by W.J. Evans [13]



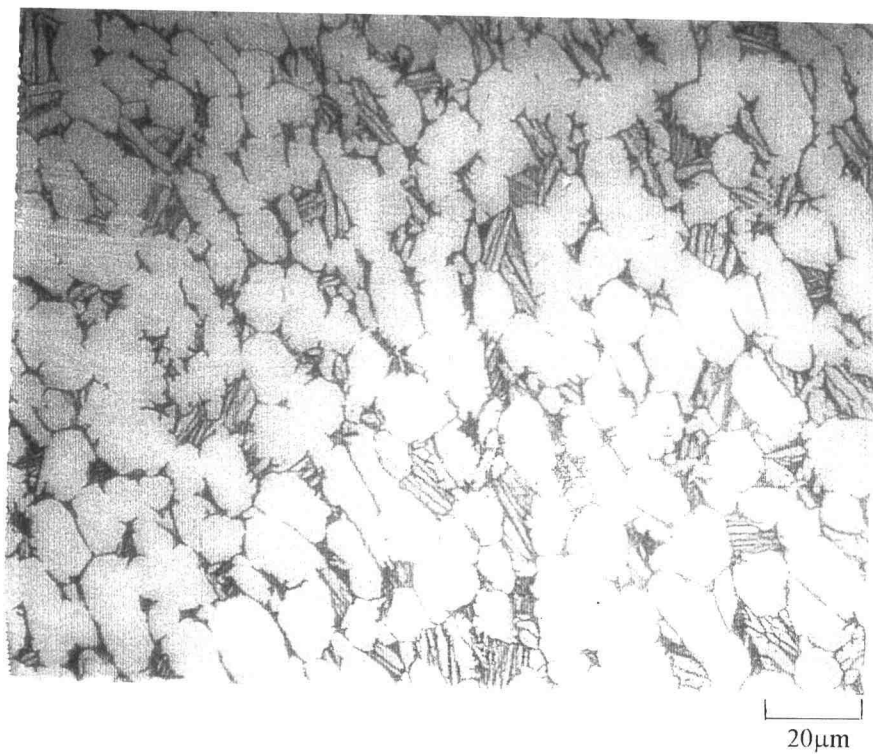


Figure 8. RT950209, Set B, Sample T2TOP1,  $T_p$  -53° C, Axial Section

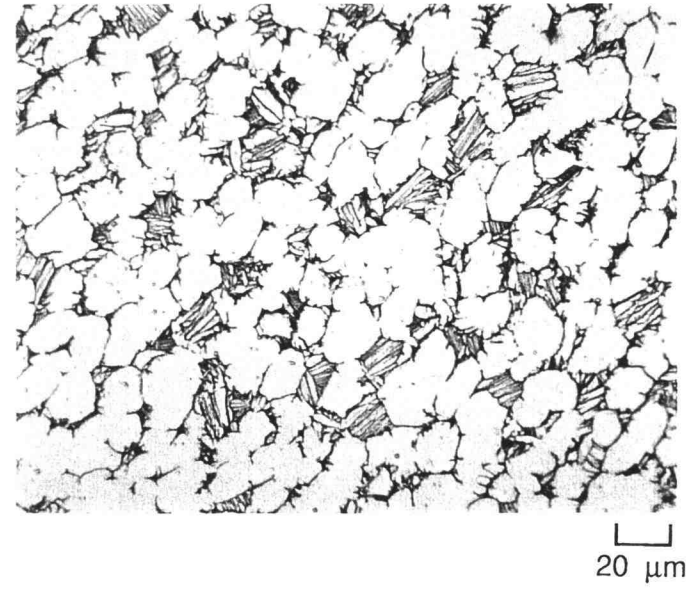
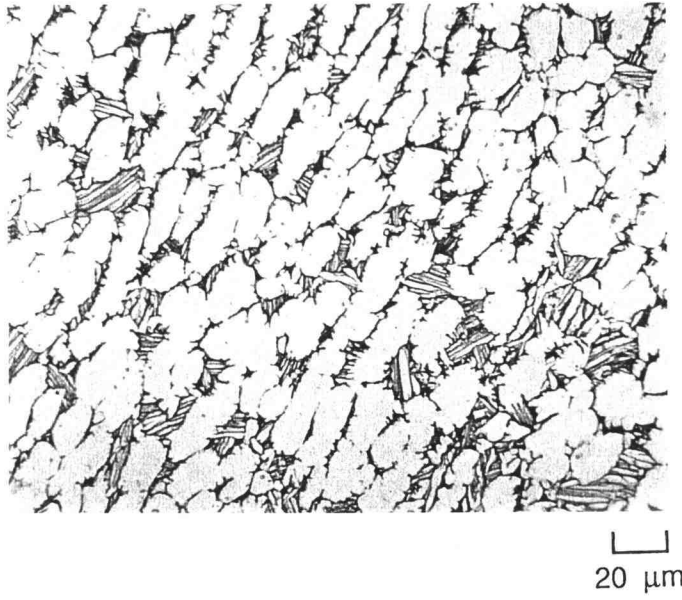


Figure 9. RT950209, Set A, Sample T2TOP4,  $T_{\beta}$   $-41^{\circ}$  C, Transverse Section

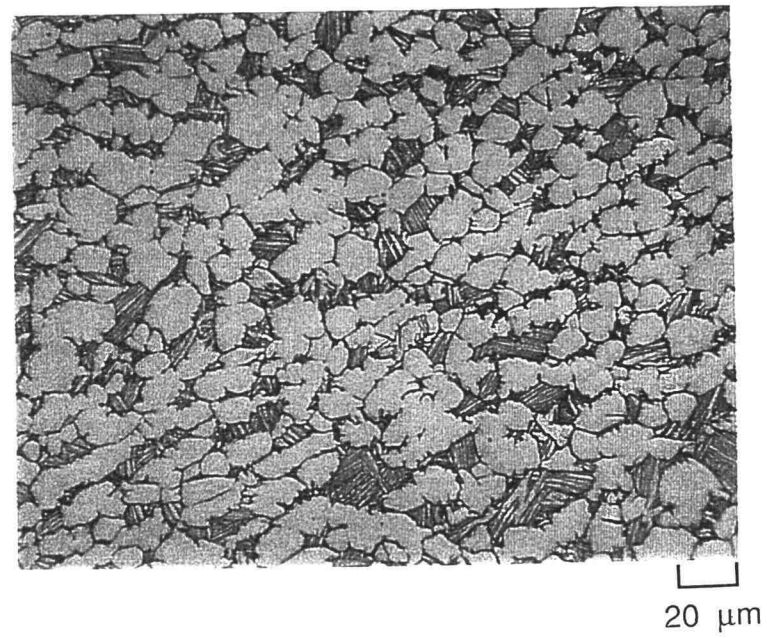
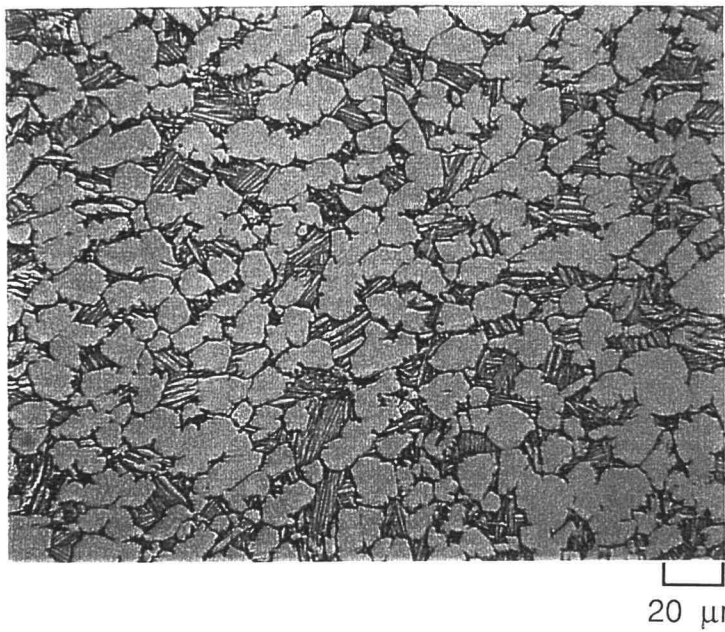
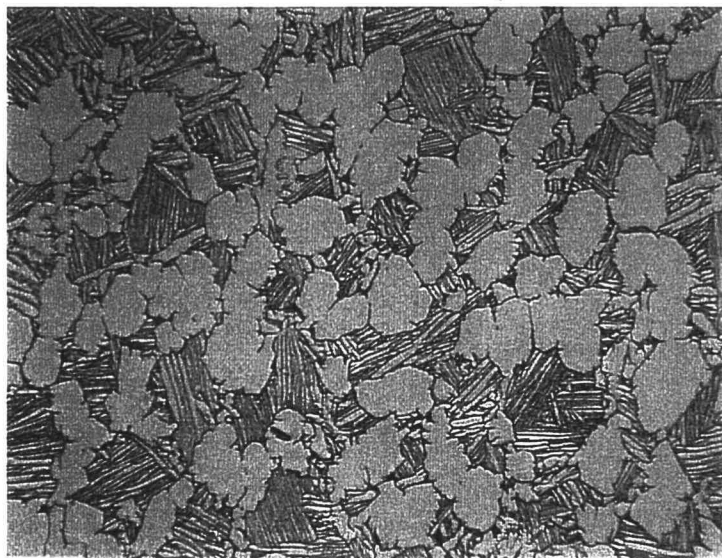
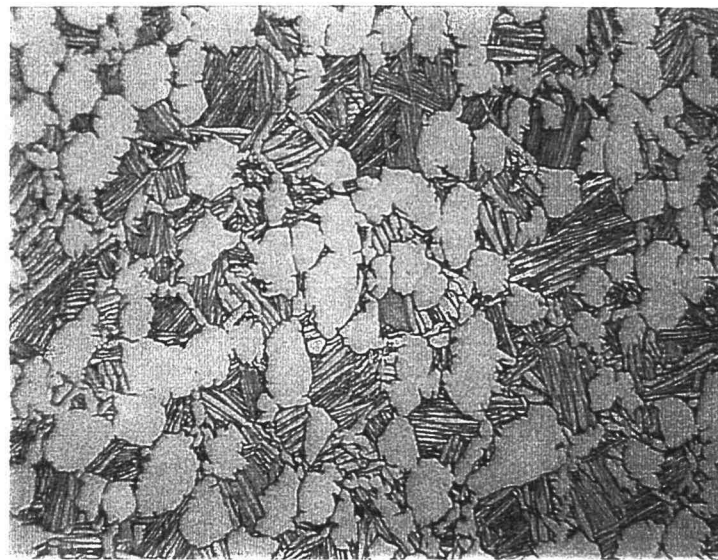


Figure 10. RT950522, Set A, Sample #2,  $T_p$  -28° C, Transverse Section





20  $\mu\text{m}$



20  $\mu\text{m}$

Figure 11. RT950483, Set A, Sample #1,  $T_{\beta}$   $-28^{\circ}\text{C}$ , Transverse Section



Figure 12. RT950209, Set B, Sample T2TOP6R,  $T_p$  -14° C, Transverse Section

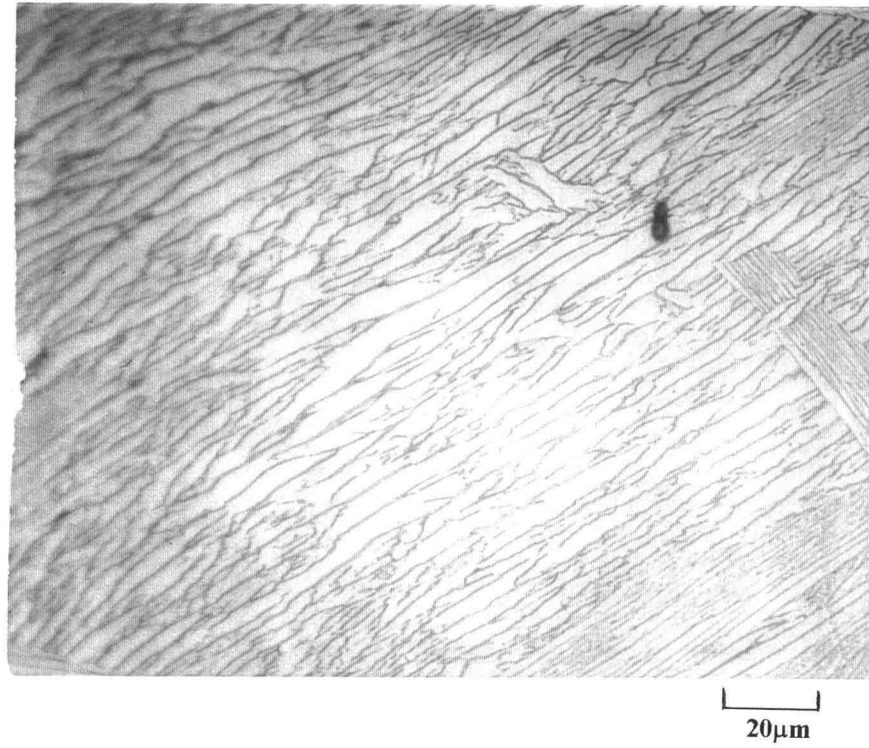


Figure 13. RT950209, Set B, Sample T2TOP22,  $T_{\beta}$  - 3° C, Transverse Section

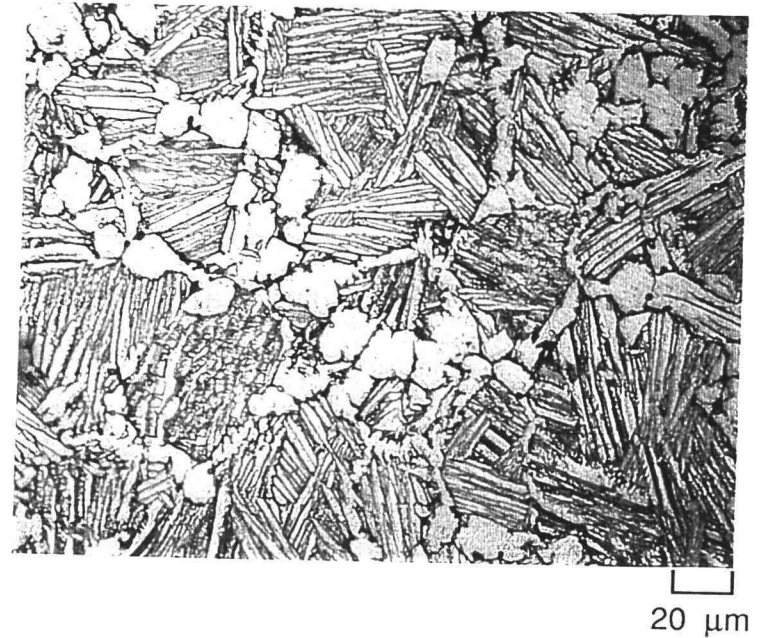
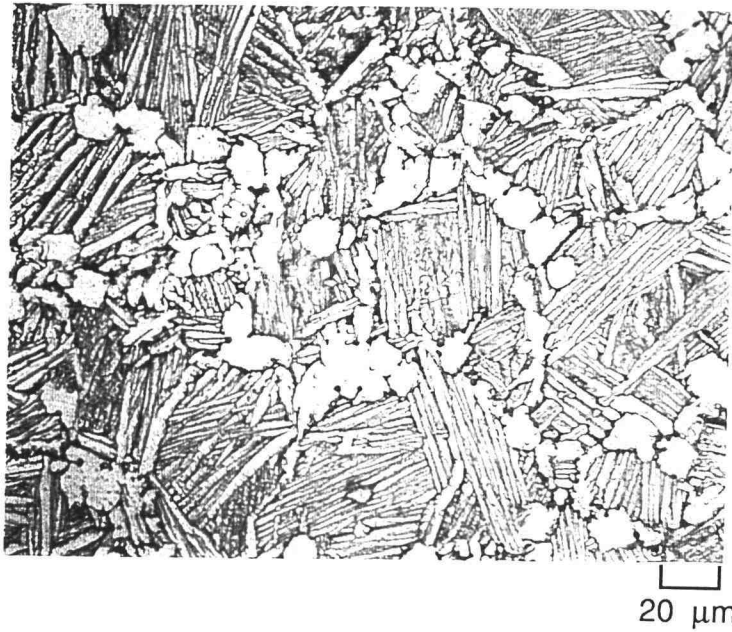


Figure 14. RT950209, Set B, Sample T2TOP18OH, Unknown Solution Anneal Temperature, Estimated  $T_{\beta}$  - 8° C, Transverse Section

**TABLE 3. SUMMARY OF AVERAGE PRIMARY ALPHA AND  
HARDNESS FOR EACH SOLUTION ANNEAL TEMPERATURE**

**Beta Transus = 1007° C**

SOLUTION ANNEAL TEMPERATURE (°C)	AVERAGE PRIMARY ALPHA PERCENTAGE	AVERAGE ROCKWELL HARDNESS (HRC)
954	65.0	no tests
966	63.0	27.6
979	54.4	30.2
993	44.2	no tests
Estimated 999	21.6	33.3
1004	5.4	31.5

Figure 15. Ti-6242S Creep Data  
(Ambient Temperature, Constant Stress Tests at 917 and 862 MPa)

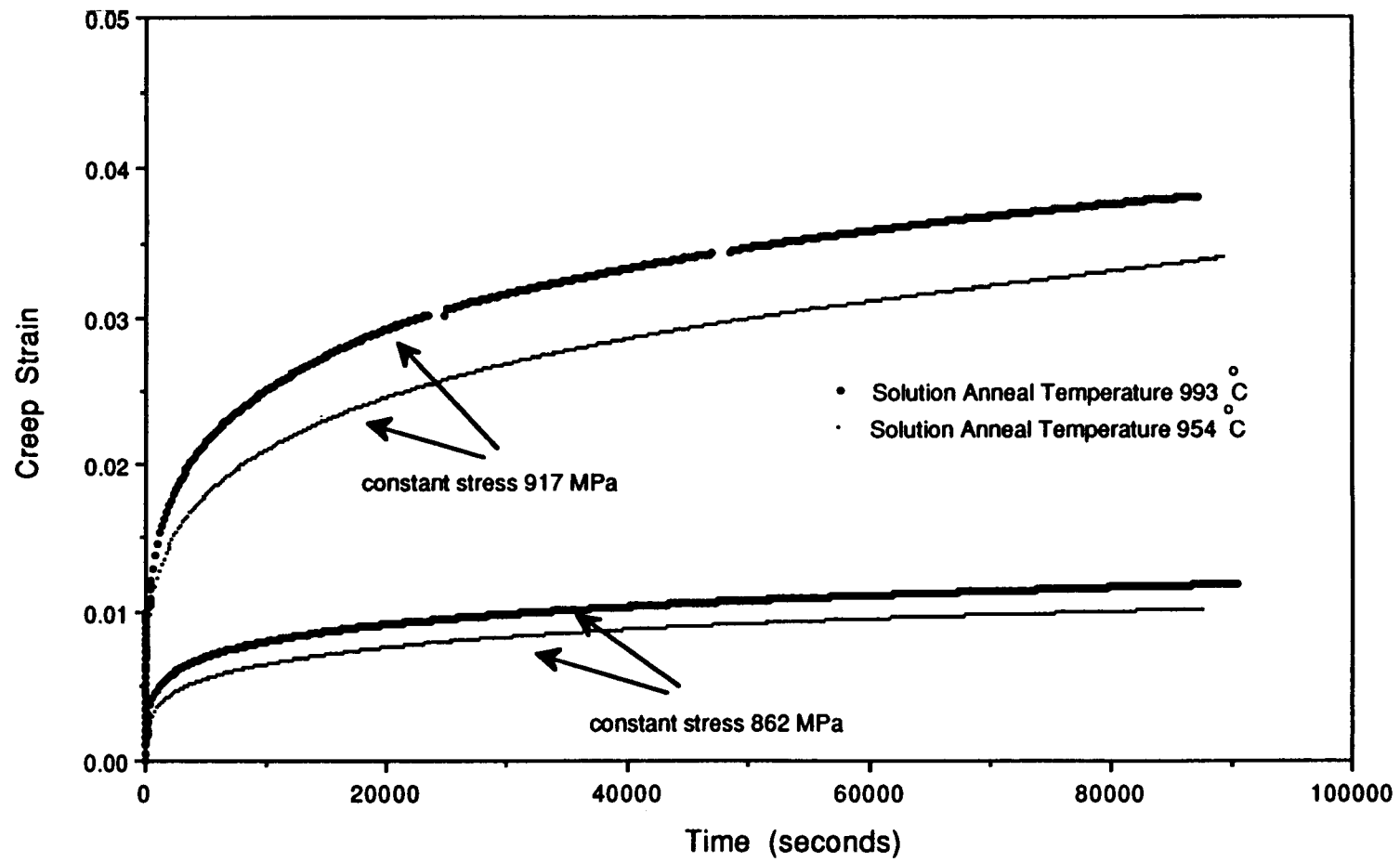


**TABLE 4. AMBIENT TEMPERATURE CREEP DATA FOR TI-6242Si<sup>1</sup>**

**Beta Transus = 1007° C**

MPa	Solution Anneal Temperature	$\epsilon_p$ at Final Load ( 63 seconds )	$\epsilon_p$ ( 120 seconds )	$\epsilon_p$ at ( $8.0 \times 10^4$ seconds )	$\dot{\epsilon}$ (s <sup>-1</sup> ) at ( $8.0 \times 10^4$ seconds )
917	T <sub><math>\beta</math></sub> -14° C	0.0082	0.010	0.037	$7.3 \times 10^{-8}$
917	T <sub><math>\beta</math></sub> -53° C	0.0064	0.008	0.033	$9.9 \times 10^{-8}$
862	T <sub><math>\beta</math></sub> -14° C	0.0011	0.003	0.012	$2.6 \times 10^{-8}$
862	T <sub><math>\beta</math></sub> -53° C	0.0005	0.002	0.010	$2.6 \times 10^{-8}$
930	T <sub><math>\beta</math></sub> -14° C	0.0105	0.013	0.054	$1.2 \times 10^{-7}$
930	T <sub><math>\beta</math></sub> -25° C	0.0047	0.006	0.025	$6.4 \times 10^{-8}$

<sup>1</sup> Two tests at 930 MPa failed during creep testing prior to  $8.0 \times 10^4$  seconds.

Tensile data as a function of solution anneal temperature for Ti-6242Si without surface shot peening is presented in Table 5. As the solution anneal temperature is increased above  $T_{\beta} - 25^{\circ}\text{C}$ , both the 0.2% offset yield strength and the ultimate tensile strength decrease with further increases in temperature.



**TABLE 5. TENSILE PROPERTIES OF TI-6242SI AS A FUNCTION OF SOLUTION ANNEAL TEMPERATURE**  
( Surfaces Not Shot Peened )

Beta Transus = 1007° C

BILLET HEAT IDENTIFICATION SAMPLE IDENTIFICATION	Solution Anneal Temperature	0.2% Yield Strength ( MPa )	UTS ( MPa )	EI ( % )	Average Hardness ( HRC )
RT950483, RT950522 A 483 #1 & #2, and A 522 #1 & #2	T <sub>β</sub> -28° C	889.4 907.4	990.8 993.5	15.0 (2) <sup>1</sup> 15.0 (2)	29.5 (10) <sup>2</sup>
RT950209 A T2TOP1 through A T2TOP14, and Manila #2	T <sub>β</sub> -41° C	879.8	979.8	14.5 (2)	27.4 (45)
RT950209 B T2TOP1 & 2	T <sub>β</sub> -53° C	882.5	972.2	16.0	————
RT950209 B T2TOP21, 22, & 23	T <sub>β</sub> -3° C	789.5	934.9	11.0	31.5 (10)
RT950209 B T2TOP1R through 13R	T <sub>β</sub> -14° C	826.0	955.6	12.0	————
RT950209 B T2TOP7OH through 20OH,	Beta Transus possibly exceeded. Most samples returned untested.	————	————	————	————

Data provided by OREMET - WAH CHANG

<sup>1</sup> Number of tests

<sup>2</sup> Number of tests per sample x number of samples tested

## DISCUSSION

Chu et al., Bania and Hall, and Hall's findings may correlate well with the greater dwell cycle fatigue resistance of Ti-6242Si specimens annealed at higher solution anneal temperatures and tested during this investigation [11, 17, 18]. As mentioned previously, Chu and coworkers found that prior ambient temperature creep works to improve low cycle fatigue life by a factor of two or more in Ti-621/0.8 (also an alpha-beta alloy) as a result of stable dislocation networks produced which delay the onset of fatigue damage. This team also reported that a dwell period at peak load in lieu of prior creep elicited the same outcome with fifty or more cycles between hold periods, but that only one cycle between hold times resulted in a reduction in fatigue life. As reported by Bania and Hall and Hall alone, "the range of primary alpha content in Ti-6242Si will result in a minimum creep rate change of a factor of at least two,"<sup>6</sup> and the high temperature (510° C) creep rate is generally reduced as the volume fraction of equiaxed primary alpha is reduced (increased solution anneal temperature) [17, 18]. Therefore, the reduced dwell sensitivity at lower volume percentages of primary  $\alpha$  may be a function of a reduced creep rate, and not a result of easier crack propagation through the primary  $\alpha$  phase.

Since microstructure (varying volume percentages of primary  $\alpha$ ) was found to have no significant effect on LCF life (Figure 6), this may be indicative of cyclic work hardening of each microstructure to approximately the same load level during load controlled tests.

Referring to Table 4 and Figures 6 and 15, significant time-dependent plasticity occurs at the higher stresses which are also associated with the greatest dwell sensitivity. This “extra” plasticity, according to Chu et al. and Hall, delays the onset of fatigue cracking [11, 18]. Again referring to Chu and coworkers’ findings, it appears that small amounts of initial monotonic deformation do not degrade the LCF properties. “Thus, the effect of the dwell may be that of repeated (cyclic) plasticity due to creep during the dwell periods.”<sup>7</sup>

Subsequent research using the DLCF and LCF specimens tested during the present investigation has shown that the DLCF specimens accumulated more plastic strain to failure than the LCF specimens due to creep plasticity [19]. Therefore, the dwell may simply increase the “strain amplitude” of a LCF test at a given stress, resulting in a decreased number of cycles to failure. It was also shown that prior monotonic creep strain comparable to that accumulated in DLCF specimens did not significantly degrade LCF life [19]. These results concur with those reported by Chu et al. [11].

One possibly important point to note is that, based on the tensile and hardness data in Table 5, the tensile strength of Ti-6242Si is approximately independent of the solution anneal temperature (or primary alpha content) up to approximately  $T_{\beta}-28^{\circ}\text{C}$ . Above

---

<sup>6</sup> P.J. Bania and J.A. Hall, *Titanium Science and Technology*, Vol. 4, Proceedings of the 5<sup>th</sup> International Conference on Titanium, Munich, 1984, p. 2371.

<sup>7</sup> M.E. Kassner, R. Faber, X. Li, Y. Ge, Y. Kosaka, S.H. Reichman, and J.A. Hall, *TMS Conference 1998*, to be published, D. Eylon, R.R. Boyer, and G. Lütjering, eds., Warrendale, 1999.

this temperature, the yield strength (YS) and ultimate tensile strength (UTS) decrease with increasing solution anneal temperature. The increased creep strain with increasing solution anneal temperature experienced during the ambient temperature creep tests is not then surprising. This trend was also observed by Suri et al. [20]. High temperature creep tests on this alloy reveal the opposite trend [21].

It appears that in the alpha-beta titanium alloys studied, most of the fatigue life is spent nucleating detectable cracks [18], as with most metals. Thus, bulk plasticity trends associated with changes in dwell cycle fatigue and low cycle fatigue may be directly related to crack nucleation. Earlier work by Kansal et al. suggests that with increased primary alpha, textured or “aligned” primary alpha becomes more obvious [22]. Chu and co-researchers’ studies showed that both creep and fatigue crack propagation did not coincide with the  $\alpha$ - $\beta$  interfaces, but propagated transgranularly (through the grains) across the  $\alpha$ - $\beta$  colonies.

Metallographic examination of a Ti-6242Si sample loaded to 876 MPa during DLCF testing, revealed that dwell cycle fatigue cracks exist in many locations away from the principal crack, and may not be associated with secondary cracks. These cracks appear to nucleate in the primary alpha phase, and appear to propagate across (transgranularly) the primary alpha grains [19]. It does not appear that the cracking is associated with the “banding” often associated with Ti-6242Si with higher volume percent primary alpha [22, 23, 24]. This banding could be associated with texture.

## CONCLUSIONS

Ambient temperature dwell and low cycle fatigue tests were performed on Ti-6AL-2Sn-4Zr-2Mo-0.1Si (Ti-6242Si). Specimens were solution annealed at various temperatures below the beta transus to vary the volume fraction of primary alpha. The influence of the changes in primary alpha phase on dwell time low cycle fatigue (DLCF) life were determined and compared to the conventional low cycle fatigue (LCF) properties of the alloy. It was concluded that:

1. A dwell significantly decreased the number of cycles to failure.
2. Increasing primary alpha, associated with lower solution anneal temperatures, significantly increased susceptibility to dwell fatigue, although this affect diminished with decreasing stress.
3. The above trends may be explained by ambient temperature, cyclic creep of Ti-6242Si.
4. Increased susceptibility of higher primary alpha to dwell fatigue may be due to an increased susceptibility of primary alpha to cracking during creep deformation.

## REFERENCES

1. C. Andres, L. Wagner, and G. Lütjering, *Microstructure/Property Relationships in Titanium Aluminides and Alloys*, Y.W. Kim and R.R. Boyer, eds., TMS, Warrendale, 1991, pp. 579-586.
2. E.W. Collings, *Physical Metallurgy of Titanium Alloys*, ASM, Metals Park, OH, 1984.
3. R.R. Boyer, *Titanium and Titanium Alloys*, Metals Handbook, 9<sup>th</sup> Edition, Vol.7, ASM, Metals Park, OH, 1982, pp. 458-475.
4. S.L. Semiatin, J.F. Thomas, Jr., and P.Dadras, *Metall. Trans.*, 14A, 1983, pp. 2363-2374.
5. A.P. Woodfield, M.D. Gorman, R.R. Corderman, J.A. Sutliff, and B. Yamrom, *Titanium '95 Science and Technology*, C.A. Bienkinsop, W.J. Evans, and H.M. Flower, eds., Institute of Materials, Cambridge Univ. Press, 1996, pp. 1116-1123.
6. W.J. Evans, *Second International Conference on Creep and Fracture of Engineering Materials and Structures, Proceedings of the Second International Conference on Creep and Fracture of Engineering Materials and Structures*, Swansea, 1984, p. 395.
7. D.R. Askeland, *The Science and Engineering of Materials*, 3<sup>rd</sup> Edition, PWS Publishing Company, Boston, 1994.
8. W.J. Evans, *J. Mater. Sci. Lett.*, 6, 1987, pp. 571-574.
9. D. Eylon and J.A. Hall, *Metall. Trans.*, 8A, 1977, pp. 981-990.
10. W.J. Evans and C.R. Gostelow, *Metall. Trans.*, 10A, 1979, pp. 1837-1846.
11. H.P. Chu, B.A. MacDonald, and O.P. Arora, *Titanium Science and Technology*, Vol. 4, G. Lütjering, U. Zwicker, and W. Bunk, eds., *Proceedings of the 5<sup>th</sup> International Conference on Titanium*, Duetsche Gesellechat für Metallkunde E.V., 1984, pp. 2395-2402.
12. J.E. Hack and G.R. Leverant, *Metall. Trans.*, 13A, 1982, pp. 1729-1738.
13. J.A. Bannantine, J.J. Comer, J.L. Handrock, *Fundamentals of Metal Fatigue Analysis*, Prentice-Hall, Englewood Cliffs, NJ, 1990.
14. S. Suresh, *Fatigue of Materials*, E.A. Davis, I.M. Ward, eds., Cambridge University Press, Cambridge, 1992.
15. D.F. Neal, *Sixth World Conference on Titanium*, Vol.1, Proceedings of the Sixth World Conference on Titanium, Cannes, 1988, pp. 175-180.

16. ASM Committee on Shot Peening, *Metals Handbook*, 9<sup>th</sup> Edition, ASM, Vol. 5, 1982, pp. 138-149.
17. P.J. Bania and J.A. Hall, *Titanium Science and Technology*, Vol. 4, *Proceedings of the 5<sup>th</sup> International Conference on Titanium*, Munich, 1984, pp. 2371-2378.
18. J.A. Hall, *Int. J. Fatigue*, Vol. 19, Supp. No. 1, 1997, pp. S23-S37.
19. M.E. Kassner, R. Faber, X. Li, Y. Ge, Y. Kosaka, S.H. Reichman, and J.A. Hall, *TMS Conference 1998*, to be published, D. Eylon, R.R. Boyer, and G. Lütjering, eds., TMS, Warrendale, 1999.
20. S. Suri, T. Neeraj, G.S. Daehn, D.H. Hou, J.M. Scott, R.W. Hayes, and M.J. Mills, *Materials Science and Eng.*, A234-236, 1997, pp. 996-999.
21. K.E. Thiehsen, M.E. Kassner, J. Pollard, D.R. Hiatt, and B.M. Bristow, *Metall. Trans.*, 24A 1993, pp. 1819-1826.
22. U. Kansal, M.E. Kassner, D.R. Hiatt, and B.M. Bristow, *J. Mater. Eng. and Perf.*, 1, 1992, pp. 393-398.
23. S.L. Semiatin and G.D. Lahoti, *Metall. Trans.*, 14A, 1983, pp. 105-115.
24. S.L. Semiatin and G.D. Lahoti, *Metall. Trans.*, 14A, 1983, pp. 743-750.
25. C. Quesne, C. Duong, F. Charpentier, J.F. Fries, and P. Lacombe, *Journal of the Less-Common Metals*, Vol. 68, 1979, pp. 133-142.
26. A. Tahmassebi Khadem Assadi, H.M. Flower, D.R.F. West, *Met. Technol.*, Jan. 1979, pp. 16-23.
27. W.J. Evans and G.F. Harrison, *Journal of Materials Science*, 18, 1983, pp. 3449-3455.
28. W. Cho, J.W. Jones, J.E. Allison, and W.T. Donlon, *Sixth World Conference on Titanium, Vol.1, Proceedings of the Sixth World Conference on Titanium*, Cannes, 1988, pp. 187-192.
29. T. Bui-Quoc, R. Gomuc, A. Biron, H.L. Nguyen, R.N. Tadros, *Journal of Testing and Evaluation*, JTEVA, Vol. 18, No. 3, May 1990, pp. 160- 171.
30. W.J. Evans and M.R. Bache, *Titanium '92 Science and Technology*, F.H. Froesand, I. Caplan, eds., TMS, 1993, pp. 1693-1699.
31. W.J. Evans and M.R. Bache, *Fatigue*, 16, 1994, pp. 443-453.
32. D. Eylon and C.M. Pierce, *Metall. Trans.*, 7A, 1976, pp. 111-121.

33. N.E. Paton and M.W. Mahoney, *Metall. Trans.*, 7A, 1976, pp. 1685-1689.



## APPENDIX

Figure 16. DCF / LCF / Creep Testing Sample Dimensions / Specifications

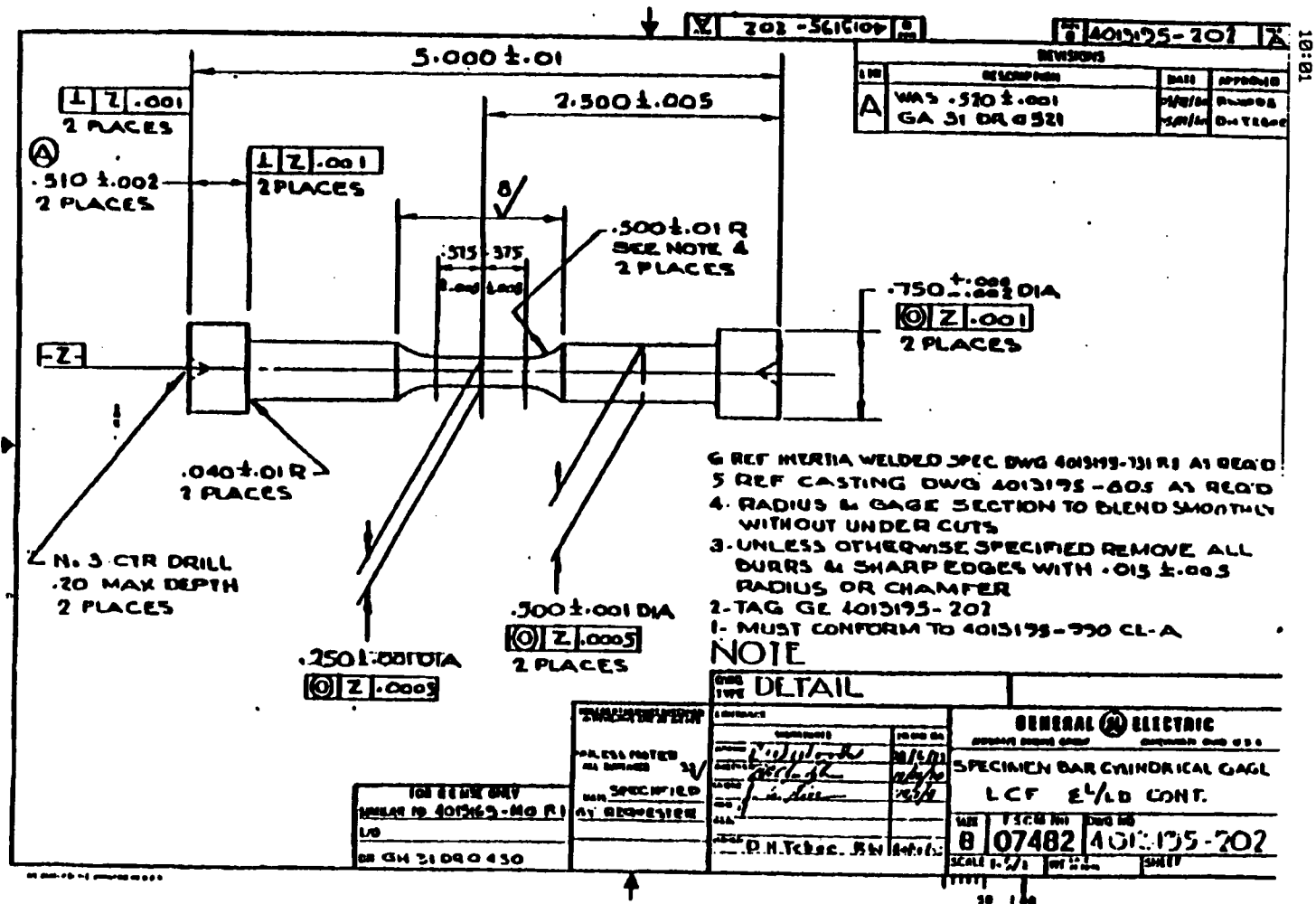


Figure 17. DCF Sampling, Preparation, and Testing Outline

## Dwell Fatigue Testing of Billet

### Sampling

Specimens for fatigue tests shall be taken at top, middle, and bottom locations at least two diameter lengths from billet ends. Two specimens are required at each location. Specimen orientation shall be radial with the gage centered approximately at the midradius position.

Sample material provided for the alternate crystallographic structure analysis shall be a single heat treated transverse slice from each of the billet locations listed above.

### Specimen Preparation

Sample material shall be solution treated at 50°F below the <sup>Beta</sup>heat (approx. 1800°F) transus temperature  $\pm 25^\circ\text{F}$  for 1 hour. Cool at  $30 \pm 5^\circ\text{F}/\text{min.}$  to below 1000°F. Age 8 hours at  $1100 \pm 15^\circ\text{F}$ .

Test bars shall have a nominal gage diameter of .25 inches and gage length of .75 inches. Gage area shall be peened using S-110, S-170, CW14, or CW33 shot to .002 - .008A. Coverage 100 to 400%.

(sample specimen drawing can be added if helpful)

### Test Conditions

Bars shall be dwell LCF tested to failure in load control. Report cycles to failure.

Temperature:	Room temperature
A-ratio:	.9 - 1.0
Peak Stress:	126 KSI
Cyclic Rate:	2 minute dwell at peak stress
Load and Unloading Rate:	1 - 3 seconds

Figure 18. Plot of Set A and Metcut Research, Inc.  
Dwell Cycle Fatigue Data

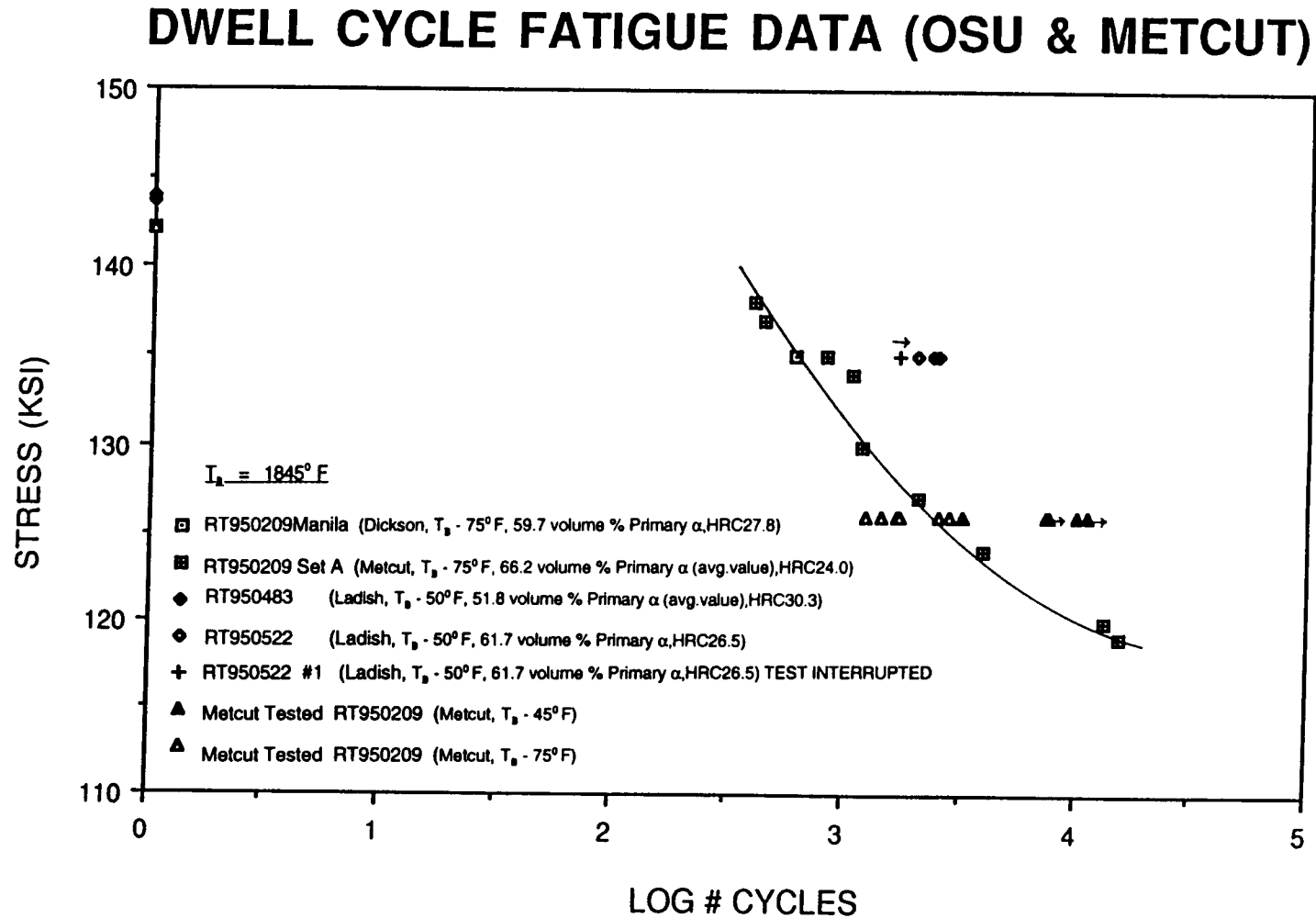


Figure 19. Ti-6242Si, Heat RT950209  
Solution Anneal Temperatures vs UTS

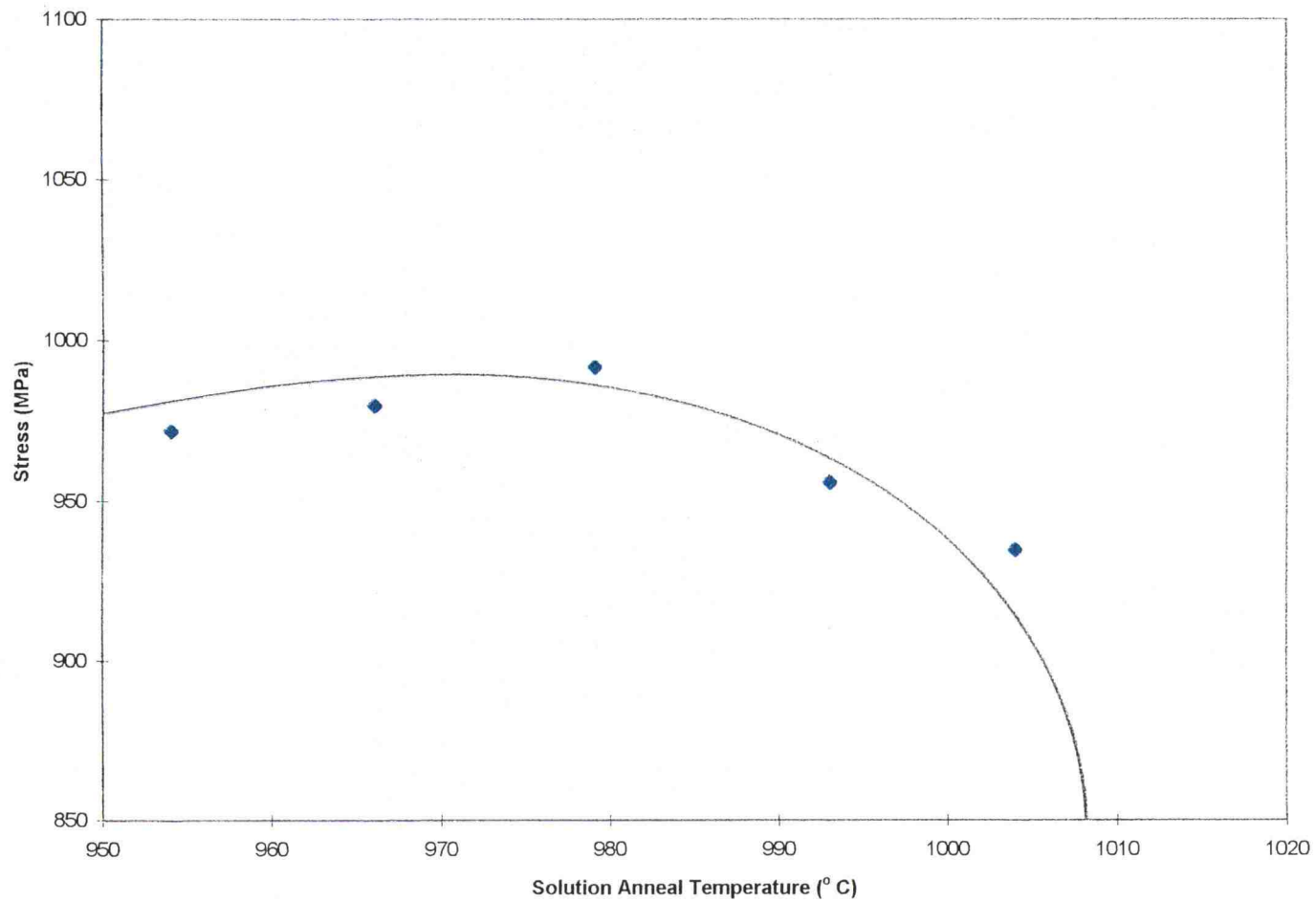


Table 6. OREMET-WAH CHANG, TI - 6242Si Specimen List & Data							
BETA TRANSUS = 1845° F = 1007° C							
SET A (Includes RT950209, samples T2TOP1 through T2TOP14, RT950209Manila, RT950483, & RT950522)							
SAMPLE ID	TYPE TEST & STRESS (KSI & MPa)		LOG # CYCLES TO FAILURE	VOLUME % PRIMARY ALPHA		ROCKWELL C HARDNESS	SOLUTION ANNEAL TEMPERATURE ( °C and °F )
T2TOP1face	DCF 135	930.8	2.91	68.2		25.9	966 1770
T2TOP1axial	DCF 135	930.8	2.91	63.4		25.9	966 1770
T2TOP2face	DCF 134	923.9	3.02	69.3		29.7	966 1770
T2TOP2axial	DCF 134	923.9	3.02	63		29.7	966 1770
T2TOP 4face	DCF 138	951.5	2.59	65.5		25.4	966 1770
T2TOP 5face	DCF 137	944.6	2.64	64.2		28.8	966 1770
T2TOP 5axial	DCF 137	944.6	2.64	58.9		28.8	966 1770
T2TOP 6face	DCF 130	896.3	3.07	66.6		27.1	966 1770
T2TOP 6axial	DCF 130	896.3	3.07	61.7		27.1	966 1770
T2TOP 7face	DCF 127	875.6	3.31	64.8		29.3	966 1770
T2TOP 8face	DCF 120	827.4	4.12	63.9		20.7	966 1770
T2TOP 8axial	DCF 120	827.4	4.12	62.6		20.7	966 1770
T2TOP 9face	DCF 124	855.0	3.60	56.3		33.6	966 1770
T2TOP 9axial	DCF 124	855.0	3.60	56.9		33.6	966 1770
T2TOP10	LCF 138	951.5	3.88				966 1770
T2TOP11	LCF 130	896.3	4.07				966 1770
T2TOP12	LCF 120	827.4	4.82				966 1770
T2TOP13	DCF 119	820.5	4.19				966 1770
T2TOP14	LCF 115	792.9	4.99				966 1770
MANILA #2face	DCF 135	930.8	2.78	59.7		27.8	966 1770
RT950483 #1face	DCF 135	930.8	3.37	53.9		27.1	979 1795
RT950483#1axial	DCF 135	930.8	3.37	45.0		27.1	979 1795
RT950483 #2face	DCF 135	930.8	3.39	49.7		33.5	979 1795
RT950522 #1face	DCF 135	930.8	3.22	TEST INTERRUPTED	61.9	33.7	979 1795
RT950522 #2face	DCF 135	930.8	3.30		61.7	26.5	979 1795

Table 7. OREMET-WAH CHANG, Ti - 6242Si Specimen List & Data (con't)								
BETA TRANSUS = 1845° F = 1007° C								
SET B (Includes RT950209B 1, 2 & 3, 21, 22, 23, 1R through 13R, 7OH through 11OH, 18OH & 19OH)								
TYPE TEST &		LOG # CYCLES		VOLUME %		ROCKWELL C	SOLUTION ANNEAL	
SAMPLE ID	STRESS (KSI & MPa)		TO FAILURE		PRIMARY ALPHA		HARDNESS	TEMPERATURE ( °C and °F)
T2TOP1face	Creep 133	Creep 917	24.1 hours		64.1		954	1750
T2TOP1axial	Creep 133	Creep 917	24.1 hours		64.0		954	1750
T2TOP2face	Creep 125	Creep 862	24.1 hours		68.1		954	1750
T2TOP2axial	Creep 125	Creep 862	24.1 hours		69.1		954	1750
T2TOP3							954	1750
T2TOP21face	DCF 135	930.8	3.33		4.16	34.5	1004	1840
T2TOP21axial	DCF 135	930.8	3.33		11.04	34.5	1004	1840
T2TOP22face	DCF 127	875.6	3.67	Test	1.53		1004	1840
T2TOP22axial	DCF 127	875.6	3.67	Interrupted	5.01		1004	1840
T2TOP23face	DCF 120	827.4	4.20		5.21	28.5	1004	1840
T2TOP23axial	DCF 120	827.4	4.20			28.5	1004	1840
T2TOP1Rface	LCF 110	758.4	5.23				993	1820
T2TOP1Raxial	LCF 110	758.4	5.23				993	1820
T2TOP2Rface	LCF 138	951.5	3.61				993	1820
T2TOP2Raxial	LCF 138	951.5	3.61				993	1820
T2TOP3R	nonconforming sample, used as dummy for creep tests						993	1820
T2TOP4Rface	LCF 135	930.8	3.77				993	1820
T2TOP4Raxial	LCF 135	930.8	3.77				993	1820
T2TOP5Rface	DCF 127	875.6	3.72		57.8		993	1820
T2TOP5Raxial	DCF 127	875.6	3.72		48.1		993	1820
T2TOP6Rface	DCF 135	930.8	3.01		39.9		993	1820
T2TOP6Raxial	DCF 135	930.8	3.01		31.1		993	1820
T2TOP7Rface	DCF 120	827.4	4.12				993	1820
T2TOP7Raxial	DCF 120	827.4					993	1820
T2TOP8Rface	DCF 138	951.5	2.66				993	1820
T2TOP8Raxial	DCF 138	951.5	2.66				993	1820

Table 7 (con't). OREMET-WAH CHANG, Ti - 6242Si Specimen List & Data								
BETA TRANSUS = 1845 °F = 1007 °C								
SET B (Includes RT950209B 1, 2 & 3, 21, 22, 23, 1R through 13R, 7OH through 11OH, 18OH & 19OH)								
(continued)								
SAMPLE ID	TYPE TEST & STRESS (KSI & MPa)		LOG # CYCLES TO FAILURE		VOLUME % PRIMARY ALPHA		ROCKWELL C HARDNESS	SOLUTION ANNEAL TEMPERATURE ( °C and °F)
T2TOP9Rface							993	1820
T2TOP9Raxial							993	1820
T2TOP10Rface							993	1820
T2TOP10Raxial							993	1820
T2TOP11Rface							993	1820
T2TOP11Raxial							993	1820
T2TOP12Rface	Creep 125	Creep 862	24.1 hours				993	1820
T2TOP12Raxial	Creep 125	Creep 862	24.1 hours				993	1820
T2TOP13Rface	Creep 133	Creep 917	24.1 hours				993	1820
T2TOP13Raxial	Creep 133	Creep 917	24.1 hours				993	1820
T2TOP7OHface	LCF 138	951.5	3.87					
T2TOP7OHaxial	LCF 138	951.5	3.87					
T2TOP8OHface	LCF 130	896.3	4.2					
T2TOP8OHaxial	LCF 130	896.3	4.2					
T2TOP9OHface	LCF 120	827.4	4.77					
T2TOP9OHaxial	LCF 120	827.4	4.77					
T2TOP10OHface	LCF 110	758.4	5.2	failed in grip				
T2TOP10OHaxial	LCF 110	758.4	5.2	failed in grip				
T2TOP11OHface	LCF 108	744.6	5.19	failed in grip				
T2TOP11OHaxial	LCF 108	744.6	5.19	failed in grip				
T2TOP18OHface	DCF 127	875.6	3.88		20.3	33.3		
T2TOP18OHaxial	DCF 127	875.6	3.88		22.8	33.3		
T2TOP19OH	Defective Surface							